The 8th International Conference on Jets, Wakes and Separated Flows, ICJWSF-2024
September 23-25, 2024, Firenze, Italy

Quantitative Flow Visualization of Supersonic Jets from an Axisymmetric Laval Nozzle by MZI

H. Ueno[1*], R. Fukunaga[1], S. Nakao[1], and Y. Miyazato[1],

1: Dept. of Mechanical Systems Engineering, The University of Kitakyushu, Japan

* Corresponding author: u.hiromu3150@gmail.com

Abstract

Slightly underexpanded free jet issuing from an axisymmetric Laval nozzle is quantitatively visualized by Mach-Zehnder interferometry. The test nozzle has an inner diameter of 15 mm at the exit and a design Mach number of 1.5. Flow visualization is performed at a nozzle pressure ratio of 5.0 to produce weak shocks. The Reynolds number based upon the diameter and flow properties at the nozzle exit is 1.15×10^6. Interferograms of underexpanded jets are taken by Mach-Zehnder interferometry with the finite fringe setting. The jet density field is reconstructed by the Abel inversion method. The flow features of time-mean density field of the jet are demonstrated.

Keywords:*Axisymmetric Laval nozzle, Mach-Zehnder interferometry, Shock wave, Supersonic jet.*

1. Introduction

Axisymmetric supersonic jets are relevant to aerospace engineering applications such as exhaust and plumes of aircrafts and rockets. In other areas, their applications can be recognized for various devices including the gas atomization for the breakup of droplets of Newtonian and non-Newtonian liquids, the assist gas for the laser cutting of mild steel, the high-velocity oxygen fuel (HVOF) spraying and cold spray technology, the blowing of soot deposited on the surface of the heating tubes during combustion to maintain boiler efficiency, the removing of carbon dioxide in a melting furnace, the peeling of leeks before shipment in the field of agriculture, etc., where the flow velocity at the exit of the nozzle attached to such a device exceeds the speed of sound. A large number of experimental studies on supersonic jets issuing from an axisymmetric nozzle have been performed so far [1], but the shock structure inside the near-field region remains only qualitatively known because it is still difficult to obtain quantitative experimental data such as pressure, density, temperature, and velocity.

Although the schlieren technique is well known as a typical visualization method for compressible flow, it is generally capable of examining the flow field only qualitatively. This is because it captures the density gradient in the flow direction or perpendicular to the flow as two-dimensional information averaged along the line-of-sight direction. Therefore, complex integral calculations with special algorithms are required to obtain the three-dimensional density of the flow field using the schlieren method. On the other hand, laser interferometers such as Mach-Zehnder interferometry [2, 3] and digital holographic interferometry [4] provide interference fringes that are directly proportional to the density field and, unlike schlieren, do not require complex integration operations.

Supersonic jets are known to exhibit unsteady behavior with flapping and spiral modes and to generate noise associated with shock waves, but few studies have quantitatively investigated the unsteady behavior of shock waves experimentally and quantitatively in three dimensions. As a first step in the research, in the present study, the time-averaged density field of an underexpanded round jet is investigated by the Mach-Zehnder interferometry (MZI).

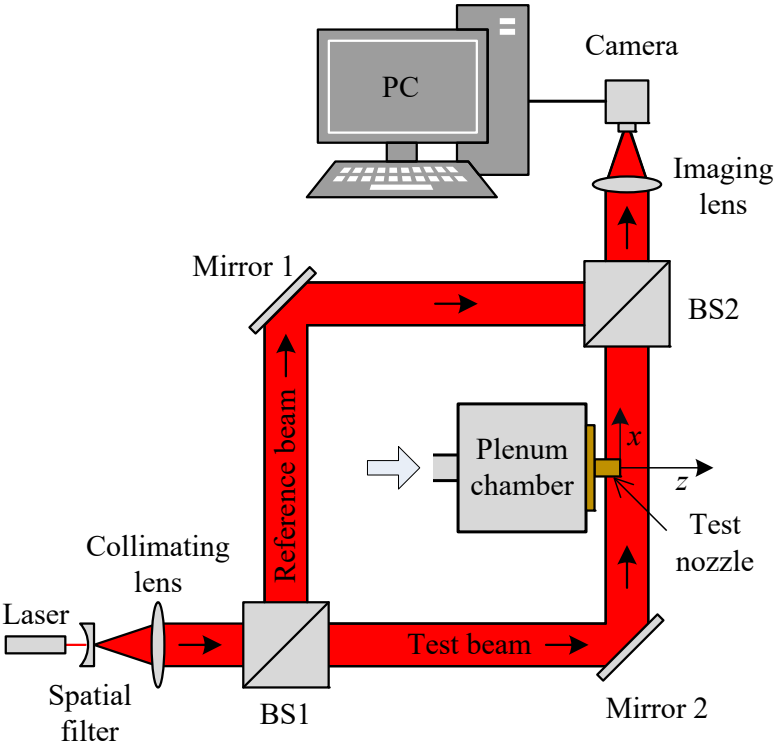

Fig. 1: Schematic diagram of the experimental apparatus with rainbow schlieren optical system

2. Experimental Methods

The experiments are conducted in an intermittent blowdown compressed-air facility. The high-pressure dry air from the reservoir is stagnated in the plenum chamber and then discharged into the quiescent air through a test nozzle. An axisymmetric Laval nozzle with an inner diameter of 15 mm at the exit and a design Mach number (M_d) of 1.5 is used as the test nozzle. The nozzle wall contour from the throat to the exit is designed by the axisymmetric method of characteristics to provide uniform and parallel flows at the nozzle exit. The density field of the jet is measured by MZI with the finite fringe setting [2, 3] at a nozzle pressure ratio (NPR) of 5.0 to produce an underexpanded jet where the NPR is defined as the ratio of the plenum chamber pressure p_{os} to the ambient pressure p_b. An ideal supersonic jet without shock waves can be achieved at NPR = 3.58 for M_d = 1.5.

A semiconductor laser with a wavelength of 633 nm is employed as a light source. In the present experiment, p_b is 101.4 kPa. The total temperature in the plenum chamber is equal to the room temperature (T_b = 291 K) during the experiment. The Reynolds number based upon the diameter and flow properties at the nozzle exit is 1.15×10^6. Interferograms of the jet density fields are captured using a digital camera with a shutter speed of 1/8000 second. The analysis of the fringe shifts relative to reference fringes is performed by the Fourier transform method and then the jet density field is reconstructed using the Abel inversion method based upon the assumption of axisymmetric flows. The spatial resolution of the present imaging system is around 92 μm in real space. In addition to the experimen, the Reynolds-averaged Navier-Stokes (RANS) simulation is performed to mutually compare with the experiment.

3. Numerical methods

The fine structure of a slightly underexpanded supersonic jet is obtained numerically using the commercial CFD software ANSYS Fluent Version 16.0. The operating condition set in the CFD code is the same as that in the experiment.

The center on the nozzle exit plane is taken as the origin (i.e., z = 0 and r = 0, where z shows the axial direction and r the radial direction). The flow is assumed to be symmetric with respect to the z-axis; therefore, only the upper half of the domain is calculated. The axisymmetric pressure-based compressible RANS equations are numerically solved. There is no universally applicable turbulence model and it should be chosen depending upon the flow condition. [4] performed the detached eddy simulation (DES) of an underexpanded

round jet with a Mach disk where the Spalart-Allmaras turbulence model was selected for the RANS areas. A comparison of the time-mean numerical density field and the experimental one reconstructed from the three-dimensional BOS was found to be in good quantitative agreement with each other. Recently, [2, 3] solved the RANS equations with the Menter's shear stress transport (SST)$k-\omega$ turbulence model to investigate shock-containing round microjets and compared the numerical results with the density field obtained from the MZI. They observed to reproduce precisely the density profiles along the three representative characteristic lines, i.e., the jet centerline, the lipline, and the intermediate line between them in the shock-cell structure. In the present simulations, the standard Menter's SST $k-\omega$ turbulence model is employed.

The inlet and ambient conditions are identical to the experimental setup (the plenum pressure , p_{os}, = 500 kPa, the plenum temperature, T_{os} = 299 K, and p_b = 100 kPa). Thus, NPR = p_{os}/p_b, is kept constant at 5.0 to produce a weakly underexpanded free jet. The dry air is assumed to follow the perfect gas law with a constant specific heat ratio of γ = 1.4, and the coefficient of viscosity is calculated by using the Sutherland's formula. The solid walls including the nozzle wall are treated as adiabatic and no-slip, and the top and right boundaries are the pressure outlets (i.e., p_b is specified). The structured mesh is generated by the mapped face meshing function equipped with ANSYS Fluent, and the total mesh count is approximately 200 thousand elements with 15 million node points. The grid spacing in the z-direction within the region from z = 0 to $7D_e$ is relatively uniform and fine (0.3 mm) in order to resolve the complex shock cell structures. Inside the nozzle, the grid size smoothly decreases in the radial direction to capture the boundary layer. The size of the smallest grids near the nozzle wall surface is around 20 μm, which corresponds to 29.4 in terms of the non-dimensional variable y^+. To accurately capture the fine structures of shock-containing jets, we set a minimum mesh interval to 0.3 mm in the vicinity of the nozzle exit. After performing a grid sensitivity analysis (not shown here), we confirm that the RANS calculation with this grid resolution can predict the flow flow-field with a reasonable agreement with the experimental data. The CFL number is set based on the pseudo transient under-relaxation method. We use the MUSCL-type finite volume schemes with the van Albada limiter to achieve the third-order accuracy in space. The spatial gradients of the flow variables are calculated in a pre-processing step at all vertices using a Green-Gauss approach and then averaged to obtain these gradients at the cell faces when computing viscous fluxes along the edges. For the time-integration, the three-stage Runge-Kutta method is used. We iterate the solution sufficiently enough so that the residuals of all equations (species, momentum, energy, turbulent kinetic energy, k, and ω) reduce by an order of three, indicating that solution seem to converge.

4. Results and Discussion

4.1. Flow visualization

An interferogram of an underexpanded jet issuing from a round Laval nozzle with a design Mach number of 1.5 under a condition of NPR = 5.0 is shown in Fig. 2(b) with the flow from left to right. For reference, Fig. 2(a) shows the interference fringes when there is no flow. The interference fringes are parallel to the radial direction in case of no flow, but when a free jet is issued from the nozzle, deformation due to shocks can be observed in the region near the nozzle exit. The oblique shock originated from the nozzle exit lip is reflected regularly on the central axis of the jet and reaches the opposite jet boundary, forming the first shock-cell.

4.2. Density contour plots

Figures 3(a) and 3(b) represent a comparison between experiment and simulation for a time-averaged density contour plot in the cross-section including the center axis of the jet. Both density fields are normalized by the ambient density ρ_b. The contour level is depicted at the top of the figure. In the experiment, the jet boundary first widens slightly just after the nozzle exit and then rapidly narrows to form the first shock-cell. The shock-cell length theoretically depends on the NPR, M_d and the specific heat ratio γ and it can be estimated by

$$\frac{L_s}{D_e} = \frac{\pi\sqrt{M_j^2-1}}{2.405}\sqrt{\frac{M_d}{M_j}}\left[\frac{(\gamma-1)M_j^2+2}{(\gamma-1)M_d^2+2}\right]^{\frac{\gamma+1}{4(\gamma-1)}} \tag{1}$$

in the normalized form [5] where M_j is the fully expanded jet Mach number [6] given by

$$M_j = \sqrt{\frac{2}{\gamma-1}\left(\mathrm{NPR}^{\frac{\gamma-1}{\gamma}}-1\right)} \tag{2}$$

and M_j = 1.71 for NPR = 5.0 of the present experiment. In the present experiment the theoretical shock-cell length leads to $(L_s/D_e)_{th}$ = 1.94 from a combination of Eqs. (1) and (2). The $(L_s/D_e)_{th}$ is found to be in good quantitative agreement with the experimental shock-cell length ($(L_s/D_e)_{ex}$ = 1.83 where the theoretical shock-cell length has an error of 6% with respect to the experimental one. Comparing the experimental and simulated density fields, both density fields are in good quantitative agreement up to the first shock-cell. However, after the first shock-cell, the jet boundary tends to decrease slightly in the flow direction in the simulation, while it is nearly constant in the flow direction in the experiment. Since this discrepancy seems to be due to the unsteady characteristics [5] of the jet, it is necessary to perform simulations that take into account the oscillations of the jet by LES instead of RAN in the future.

4.3. Streamwise density distributions

Three representative streamwise density distributions including the (a) jet centerline, (b) intermediate line, and (c) lipline are demonstrated in Fig. 4. The red and blue lines denote the experiment and simulation, respectively. The black dashed line parallel to the abscissa indicates the normalized fully expanded jet density (ρ_j/ρ_b = 1.58). The density is higher than the atmospheric density on the dashed line, but the static pressure is equal to the back pressure, and the static pressures below this line are lower than the back pressure [2].

The experimental density distributions along the central axis (a) and intermediate line (b) are signifi-

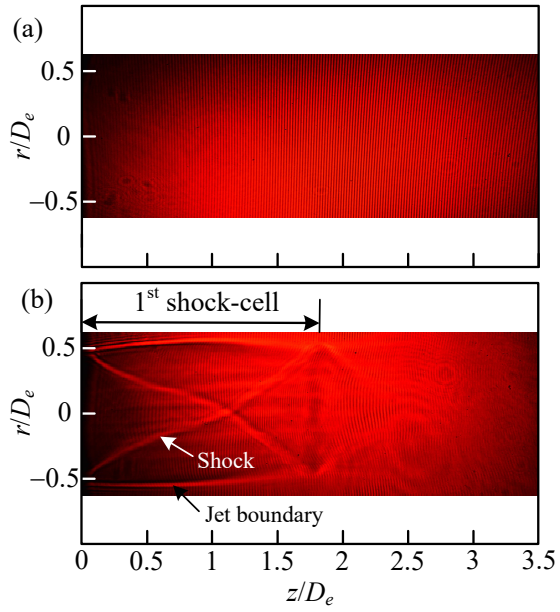

Fig. 2: Interferograms of (a) no flow and (b) an underexpanded free jet.

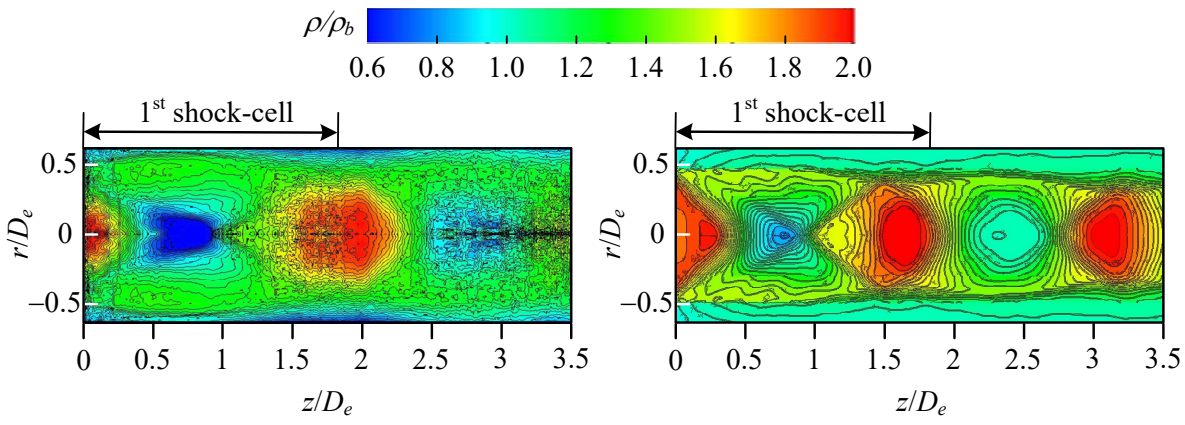

Fig. 3: Comparison between (a) experiment and (b) simulation for the density contour plot in the cross-section including the central axis of an underexpanded jet.

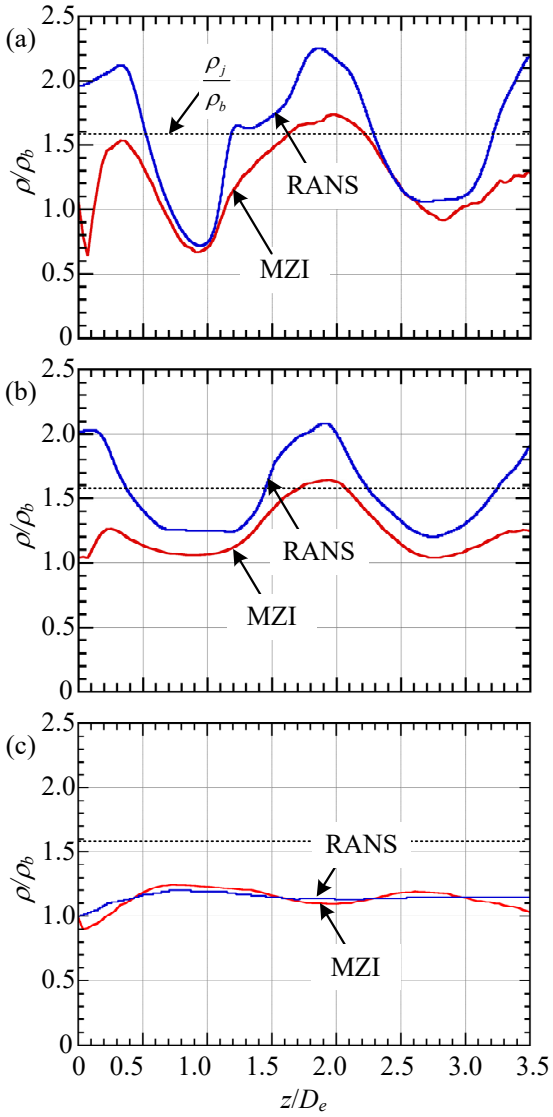

Fig. 4: Streamwise density profiles along the (a) jet centerline (r/D_e = 0), (b) intermediate line (r/D_e = 0.25), and (c) lipline (r/D_e = 0.5).

cantly lower at the nozzle exit, which are effects of light refraction at the nozzle exit cross section and not a characteristic of the jet. Due to the underexpansion jet, the density along the central axis of the jet gradually decreases from z/D_e = around 0.5 to a minimum at z/D_e = around 1.0. Downstream of z/D_e = around 1.0, the density gradually increases due to weak shocks or compression waves in the first shock-cell before reaching a peak value at z/D_e = 2.0. Subsequently, the density changes quasi-periodically in the downstream direction, similar to the density variation inside the first shock-cell. The simulated density along the jet centerline is in good quantitative agreement with the experimental one near the density minima, but elsewhere the agreement is qualitative. It should be noted here that the expansion from the nozzle exit takes place to a value considerably lower than the back pressure. The flow Mach number (M_1) and the static pressure (p_1/p_b) at the location of the density minimum can be evaluated as M_1 = 2.49 and p_1/p_b = 0.297, respectively, since it can be regarded as an isentropic change from the upstream of the nozzle to the location.

The density distribution along the intermediate line is almost a periodic increase and decrease in density in the flow direction due to the shock-cell structure. The simulated density distribution is in good qualitative agreement with the experimental one, but is generally higher than the experimental value. The density variation along the lipline is small due to the weak effects of compression waves, but the density is almost the same as the atmospheric density from the nozzle exit over the measured range. However, the static pressure remains below atmospheric. The numerical result along the lipline captures well the slight density change

due to compression waves and is in excellent quantitative agreement with the experimental one.

5. Conclusions

A slightly underexpanded free jet issuing from an axisymmetric Laval nozzle with a design Mach number of 1.5 was experimentally investigated by rainbow schlieren tomography. In addition, the Reynolds-averaged Navier-Stokes simulation was performed for mutual comparison with the experiment. The conclusions obtained are as follows.

(1) At the first density minimum in the density profile along the jet central axis, the static pressure drops to about one-third of atmospheric pressure, where the Mach number is about 2.5.

(2) Numerical simulations show good quantitative agreement with the experiment for the density variation along the lipline, but only qualitative agreement with experiments for internal density changes.

Acknowledgments

The authors thank Dr. Takeshi Miyakuni of the University of Kitakyushu for fabricating the Laval nozzle used in the experiments. This work was supported in part by Institute of Environmental Science and Technology, The University of Kitakyushu.

References

[1] Franquet E. et al. “Free Underexpanded Jets in a Quiescent Medium: A Review”. In: *Progress in Aerospace Sciences* 77 (2015), pp. 25–53.

[2] Sugawara S. et al. “Three-Dimensional Reconstruction of a Microjet with a Mach Disk by Mach-Zehnder Interferometers”. In: *Journal of Fluid Mechanics* 893 (2020), A25.

[3] Sugawara S. et al. “Quantitative Flow Visualization of Slightly Underexpanded Microjets by Mach-Zehnder Interferometers”. In: *Flow Turbulence and Combustion* 106 (3) (2021), pp. 971–992.

[4] Léon O. et al. “Three-Dimensional Density Field of a Screeching Under-Expanded Jet in Helical Mode Using Multi-View Digital Holographic Interferometry”. In: *Journal of Fluid Mechanics* 947 (2022), A36.

[5] Tam C. K. W. “Supersonic jet noise”. In: *Annual Review of Fluid Mechanics* 27 (1) (1995), pp. 17–43.

[6] Tashiro T. et al. “Flow Features of Underexpanded Microjets Emerging from a Round Convergent Nozzle”. In: *Experiments in Fluids* 64 (3) (2023), p. 55.